

## The Maximum Range of High Energy Electrons in Aluminum and Copper\*

FRANK L. HEREFORD

*Rouss Physical Laboratory, University of Virginia, Charlottesville, Virginia*

AND

CHARLES P. SWANN

*Bartol Research Foundation of the Franklin Institute, Swarthmore, Pennsylvania*

(Received January 20, 1950)

The practical maximum range of monoenergetic electrons in aluminum and copper has been measured in the region of energy from 3 to 12 Mev. The magnetically analyzed beta-ray spectrum of  $B^{12}$  was employed, range values being determined from absorption curves obtained with a triple coincidence counter train. The values so obtained fall below a semi-empirically computed curve normalized with experimental data in the region of electron energy below 3 Mev. It is shown that the discrepancy can be explained if the influence of multiple scattering effects in the absorber is considered. On this basis the data indicate that the difference between the "absolute maximum range" and the "practical maximum range" increases with electron energy.

### INTRODUCTION

THE experimental data concerning the maximum range of electrons in matter have been summarized by various workers in an attempt to establish an accurate empirical relationship between range and energy.<sup>1-3</sup> Until recently the only available measurements were in the region of energy below 3 Mev. The most complete treatment of these data is that of Bleuler and Zünti<sup>2</sup> who determine a semi-empirical curve valid in the low energy region ( $E < 3$  Mev). With regard to a beam of monoenergetic electrons they distinguish between the *absolute maximum range*,  $R_0$ , and the *practical maximum range*,  $R_p$ , which is the most conveniently measurable quantity in experiment. The absorption curves of monoenergetic electron beams (Fig. 3) in which thicknesses are measured relative to  $R_p$  indicate the significance of this quantity; it is best determined by extrapolation of the linear portion of the absorption curve through zero intensity. The *absolute maximum range*,  $R_0$ , lies to the right of this point and represents the maximum thickness penetrated by the few electrons which suffer no scattering or straggling in the absorber. It should be noted that neither of these quantities can be identified immediately with the endpoint ranges of beta-spectra where a distribution of energies is involved. Part I of this paper concerns the results of an experimental investigation of  $R_p$  in the region of energy above 3 Mev; the results are interpreted in Part II where it is shown that multiple scattering effects can account for the discrepancy between the data and previously computed values of  $R_p$ .

### PART I

A series of measurements of  $R_p$  in aluminum and copper in the region of energy from 3 to 12 Mev was

\* The experiments reported in Part I were carried out at the Bartol Research Foundation under the joint program of the ONR and AEC; the analysis and computation in Part II at the University of Virginia.

<sup>1</sup> N. Feather, Proc. Camb. Phil. Soc. 34, 599 (1938).

<sup>2</sup> E. Bleuler and W. Zünti, Helv. Phys. Acta 19, 376 (1946).

<sup>3</sup> L. E. Glendenin, Nucleonics 2, No. 1, 12 (1948).

undertaken with monoenergetic electrons and a triple coincidence counter train. The source of electrons employed was the beta-spectrum of  $B^{12}$  (produced through the  $B^{11}(d,p)B^{12}$  reaction) magnetically analyzed to provide a beam homogeneous in energy. The geometrical arrangement of the counters relative to the 90 degree magnet employed is indicated in Fig. 1. A target of  $B_2O_3$  was placed in the chamber of the Bartol Van de Graaff machine at approximately the upper focal point of the magnet, the deuteron beam being focused at this point. After traversal of the magnet chamber the analyzed electron beam emerged through a  $0.04\text{-g/cm}^2$  aluminum window to impinge upon the counters and absorbers.

In order to check the calibration of the magnet the momentum distribution of the  $B^{12}$  beta-spectrum was investigated. Comparison of the curve obtained with that of Hornyak, *et al.*<sup>4</sup> is shown in Fig. 2. It is seen that a Kurie plot of the data yields an end point at  $27.3 m_0c^2$  (13.4 Mev) in good agreement with their value, which fact is gratifying verification of the magnet calibration employed here.

In obtaining the absorption curves of the beam, double coincidences (1, 2) and triple coincidences (1, 2, 3) were recorded simultaneously with two scalars. The beam intensity penetrating each absorber thickness was taken as the triple coincidence rate relative to the

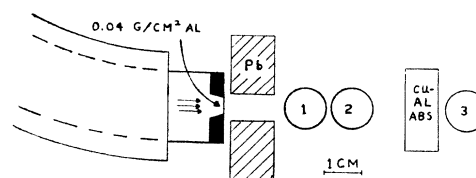


FIG. 1. The arrangement of counters and absorber relative to the magnetic analyzer. The deuteron beam was focused upon a  $B_2O_3$  target at the upper focal point of the magnet (not shown). The analyzed beta-ray beam emerged from the bending chamber as indicated.

<sup>4</sup> Hornyak, Dougherty, and Lauritsen, Phys. Rev. 74, 1727 (1948).

double, the latter rate monitoring the beam intensity hitting the absorber. By means of this scheme the aluminum absorption curves of Fig. 3 were obtained. In order to avoid confusion, no correlation is indicated between the individual points and the electron energy to which they refer. The high statistical accuracy of the counting rates and the careful determination of the various absorber thicknesses lead to an estimated probable error in each value of  $R_p$  of  $\pm 0.1$  g/cm<sup>2</sup>. The curves shown are corrected for counter wall and window thicknesses. The copper absorption curves which were very similar to those in Fig. 3 are not shown.

The similarity of the shapes of these curves to that predicted through semi-empirical calculation<sup>5</sup> is striking. At first glance the close grouping of the points beyond  $R_p$  illustrated in the insert in Fig. 3 seems to indicate that the "tails" of the curves are identical and, hence, that the difference,  $R_0 - R_p$ , is independent of energy, in agreement with the assumption of Bleuler and Züti. However, the fact that the statistical inaccuracy of these points is somewhat larger than for those measuring greater intensities lends uncertainty to this conclusion.

Values of  $R_p$  have been plotted against the corresponding electron energies in Fig. 4. The dotted curve shown was obtained from the semi-empirical expression for  $R_p$  given by Fowler *et al.*<sup>5</sup> This expression was derived through integration of the theoretical energy

loss due to ionizing collisions, normalizing the range values so computed with an experimental value at 2.96 Mev. The possible influence of multiple scattering effects on the difference,  $R_0 - R_p$ , was not considered. The solid lines shown in Fig. 4 were not drawn through the experimental points, but were computed as outlined in Part II. Two striking features of the results are: (1) the discrepancy between the experimental and computed values of  $R_p$  for aluminum above the normalization point (2.96 Mev); (2) the fact that the values of  $R_p$  for copper lie below those for aluminum. The latter is in disagreement with the relative ranges in copper and aluminum expected on the basis of ionization energy loss alone. Among the immediately evident factors bearing on this point are the increased probabilities of radiative collisions and of Coulomb scattering in copper. The influence of these real effects on the results obtained will be discussed in Part II.

The possible introduction of errors caused by several experimental difficulties, however, requires attention here. First, it is noted that the measured values of  $R_p$  are characterized by the background rate present, the counter geometry employed, and various other factors upon which  $R_p$  is heavily dependent. In particular at higher energies  $R_p$  is determined by a smaller fraction of the incident beam than at lower energies; hence, the influence of the background rate becomes more important. It is difficult to assess the magnitude of this effect. However, within the limits of accuracy of the observed counting rates beyond  $R_p$  ( $\sim \pm 8$  percent), there does not appear to be a sufficient change in the shape of the absorption curves to cause the difference between the computed and measured values of  $R_p$ .

Another possible source of experimental error is that arising from the finite resolution or window of the magnet (estimated to be four percent). Beyond the maximum of the momentum distribution (Fig. 2) the steepness of the curve might give rise to an excess of beta-rays of energy below the window midpoint over those of energy above. In the neighborhood of 10 Mev an error of 11 percent in the electron energy would be required to bring the experimental and computed values into agreement, while on the basis of the resolution estimated from geometrical considerations and subsidiary experiments, it does not seem that the average energy could differ from the window midpoint by more than two percent at the most.

It must be emphasized finally that the values of  $R_p$  reported herein can only be used in a meaningful way when proper attention is given to the geometry of the detection system. Apparent absorption due to scattering of the particles out of the solid angle subtended by the counters renders  $R_p$  sensitive to the separation and size of the counters employed. The range-energy curves given serve only as an experimental definition of  $R_p$  for the particular geometry described and for a monoenergetic source of electrons.

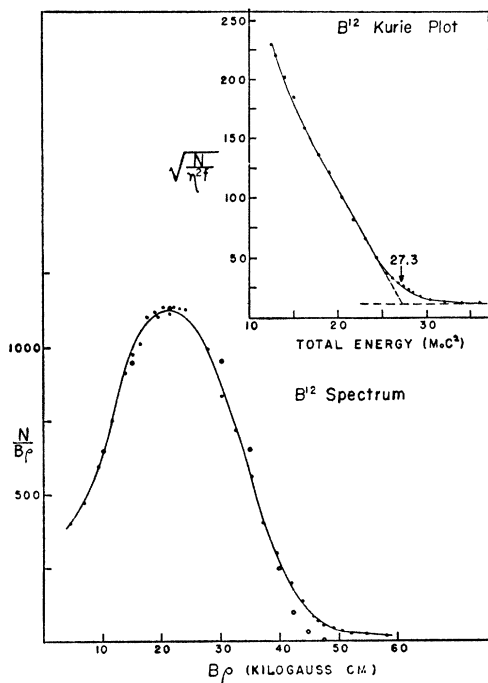


FIG. 2. The momentum distribution of the B<sup>12</sup> beta-ray spectrum. Open circles are points taken from the curve of Hornyak *et al.* (reference 4). The insert shows a Kurie plot near the end point.

<sup>5</sup> Fowler, Lauritsen, and Lauritsen, *Rev. Mod. Phys.* **20**, 237 (1948).

## PART II

In view of the disposal of the possibility of accounting for the discrepancy between the observed and computed values of  $R_p$  through the influence of experimental errors, the computation of  $R_p$  has been re-examined with regard to possible modes of range reduction in addition to ionization losses. The importance of losses increasing strongly with atomic number is evident from consideration of the relative range values observed in copper and aluminum. Contrary to expectation from ionization loss consideration, the values for copper fall below those for aluminum. Immediately obvious effects which might contribute to this state of affairs are reductions of  $R_p$  by radiative collisions and multiple scattering.

It seems very unlikely that radiative collisions could influence appreciably the value of any quantity approximating a maximum range in the region of energy involved here. The energies concerned are considerably less than the critical energies (52 Mev for aluminum, 22.4 Mev for copper), the absorber thicknesses small fractions of the radiation lengths (26.3 g/cm<sup>2</sup> for aluminum, 13.3 g/cm<sup>2</sup> for copper). Furthermore, as has been pointed out by various other workers, radiation losses generally appear as large losses by a few particles rather than small losses by many. Hence, the fraction

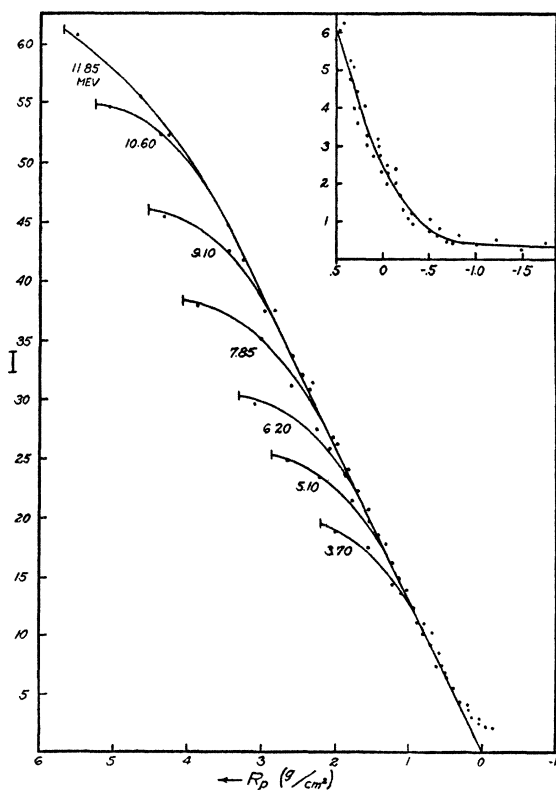


FIG. 3. Aluminum absorption curves for various electron energies. The curves are normalized at the "practical maximum range,"  $R_p$ . Intensity units are arbitrary. The insert shows the end point region on an expanded scale.

of an incident beam penetrating to a depth approaching the maximum penetration depth should not be effected.

On the other hand, no such arguments are valid as regards multiple scattering. It is normally assumed that  $R_p$  as well as the absolute maximum range,  $R_0$ , is determined by a small number of the incident electrons which have not experienced scattering in the absorber. Hence, the measured absorber thickness is identified with the trajectories of the electrons reaching both  $R_p$  and  $R_0$ . In accordance with this, the difference,  $R_0 - R_p$ , is considered to be a constant characterizing in some way the shape of the absorption curve near the end point. The screening of the nuclear field by the orbital electrons imposes a minimum value on the possible scattering angles in single collisions,<sup>6</sup> a minimum which decreases with increasing energy of the incident electron (decreasing de Broglie wave-length). This fact might be interpreted as allowing the constancy of  $R_0 - R_p$ . Such is not the case here; we are concerned with the superposition of many such small deviations which can result in any finite angle when averaged over the total path. Thus while the equivalence of trajectory and thickness holds for those few electrons reaching  $R_0$ , it cannot hold absolutely for those reaching only  $R_p$ . The difference between  $R_p$  and the trajectory length,  $R_0$ , then will be considered to be due to multiple scattering in the absorber. On this basis it would be expected to increase with increasing absorber thickness and hence with electron energy.

It is possible to take into account the effect of multiple scattering in computation of  $R_p$  by means of the semi-empirical method to follow.

We adopt g/cm<sup>2</sup> as units of range and employ the units and notation of Rossi and Greisen.<sup>7</sup> The absorber thickness,  $R_p(E)$ , expressing the practical maximum range of an electron of energy  $E$  is assumed to be less than the trajectory length,  $x(E)$ , by an amount characterized by the multiple scattering of those electrons reaching  $R_p(E)$ . We will compute  $R_p(E)$  in terms of a standard value  $R_{p0} = R_p(E_0)$  and a standard trajectory length,  $x_0 = x(E_0)$ , as follows:

$$R_p(E) = R_{p0} = \{x(E) - x_0\} \cos \bar{\theta}$$

or, since the deflections are small,

$$R_p(E) - R_{p0} = \{x(E) - x_0\} \{1 - \bar{\theta}^2/2\}. \quad (1)$$

The quantity  $\bar{\theta}^2$  is some mean-square angle of scattering suffered by those electrons which reach  $R_p$  in traversing the thickness,  $R_p - R_{p0}$  (i.e., in traveling the distance along the trajectory given by  $x - x_0$ ). It is assumed that  $\bar{\theta}^2$  is proportional to the mean-square angle of scattering of all electrons in a beam traversing  $x - x_0$ ,

$$\bar{\theta}^2 = \alpha \langle \theta^2 \rangle_{Av(x-x_0)} = \alpha \frac{E_0^2}{X_0} \int_{x_0}^x \frac{dx}{p^2 \beta^2}. \quad (2)$$

The expression for the mean-square angle of scattering

<sup>6</sup> E. J. Williams, Proc. Roy. Soc. 169, 531 (1939).

here is that given by Rossi and Greisen.<sup>7</sup>  $E_s$  is a constant (21 Mev),  $X_0$  is the radiation length in g/cm<sup>2</sup>, and  $\alpha$  is a constant to be determined.

The quantity  $x(E) - x_0$  can be computed following Fowler *et al.*<sup>5</sup> by integration of the theoretical energy loss.

$$x(E) - x_0 = \int_{E_0}^E \frac{dE}{(dE/dx)_{\text{ion}}} \quad (3)$$

We choose  $E_0$  sufficiently large to render valid the extreme relativistic (E.R.) approximation to  $(dE/dx)_{\text{ion}}$  given by Heitler,<sup>8</sup> *viz.*,

$$(dE/dx)_{\text{ion}} = \xi \ln(\gamma M),$$

where,  $W$  = total energy in Mev,

$$\xi = 6C\mu_e = \begin{cases} 0.22 \text{ Mev cm}^2/\text{g}, & \text{for aluminum,} \\ 0.21 \text{ Mev cm}^2/\text{g}, & \text{for copper,} \end{cases}$$

$$\gamma = [2\mu_e J_0^2(Z)]^{-1/2} = \begin{cases} 316 \text{ Mev}, & \text{for aluminum,} \\ 187 \text{ Mev}, & \text{for copper.} \end{cases}$$

We have then for Eq. (3),

$$x(E) - x_0 = (1/\xi) \int_{W_0}^W \frac{dW}{\ln(\gamma W)}. \quad (4)$$

In view of the choice of  $E_0$  and hence of  $W_0$  in the relativistic region, Eq. (2) may be rewritten by a change of variable, using  $W^2 = p^2 + \mu_e^2$ , and approximated as,

$$\begin{aligned} \bar{\theta}^2 &= \alpha \frac{E_s^2}{X_0} \int_{W_0}^W \frac{dW}{\beta^2(W^2 - \mu_e^2)(dE/dx)_{\text{ion}}} \\ &\approx \alpha \frac{E_s^2}{X_0 \xi} \int_{W_0}^W \frac{dW}{W^2 \ln(\gamma W)}. \end{aligned} \quad (5)$$

The integrals in Eqs. (4) and (5) can now be evaluated in terms of the exponential integrals of positive and negative argument<sup>9</sup> through introduction of  $y = \ln(\gamma W)$  leading to the results

$$\begin{aligned} x - x_0 &= (1/\xi\gamma) [Ei(\ln\gamma W) - Ei(\ln\gamma W_0)], \\ \bar{\theta}^2 &= \alpha(E_s^2\gamma/X_0\xi) [Ei(-\ln\gamma W) - Ei(-\ln\gamma W_0)]. \end{aligned}$$

With reference to Eq. (1) we have,

$$R_p(E) - R_{p0} = (1/\xi\gamma) [Ei(\ln\gamma W) - Ei(\ln\gamma W_0)] \times [1 - \alpha k \{Ei(-\ln\gamma W) - Ei(-\ln\gamma W_0)\}], \quad (6)$$

where  $k$  has been written for  $E_s^2\gamma/\xi X_0$ .

We now choose two experimental points on the  $R_p$  vs.  $E$  curve, the first as the standard range  $R_{p0}$ , the second to allow evaluation of the constant  $\alpha$ . Following

<sup>7</sup> B. Rossi and K. Greisen, *Rev. Mod. Phys.* **13**, 240 (1941).

<sup>8</sup> W. Heitler, *The Quantum Theory of Radiation* (Oxford University Press, London, 1936), p. 220.

<sup>9</sup> These functions are tabulated in the range of values pertinent here in *Tables of Sine, Cosine, and Exponential Integrals* (Work Projects Administration, New York, 1940), Vol. II.

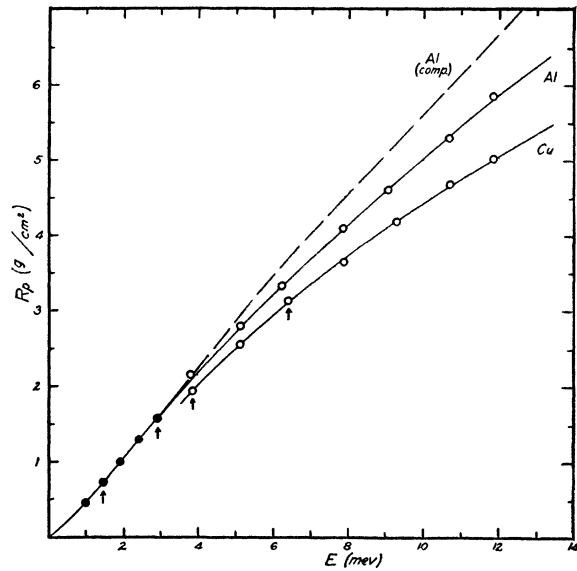


FIG. 4. Values of  $R_p$  plotted against corresponding electron energies are represented by open circles. The dotted line was plotted from the calculations of Fowler *et al.* (reference 5). Solid lines were computed by the method described in Part II of this paper. Solid points are from the summary of Bleuler and Zünti (reference 2). The arrows indicate the normalization points,  $R_{p0}$  and  $R_{p1}$  (see text).

the summary of Bleuler and Zünti,<sup>2</sup> we take for aluminum,

$$\begin{aligned} R_{p0} &= 0.70 \text{ g/cm}^2, & \text{for } W = 2.04 \text{ Mev,} \\ R_{p1} &= 0.16 \text{ g/cm}^2, & \text{for } W = 3.48 \text{ Mev.} \end{aligned}$$

In the absence of experimental data in the region of lower energies for copper we choose two points from Fig. 4,

$$\begin{aligned} R_{p0} &= 1.92 \text{ g/cm}^2, & \text{for } W = 4.30 \text{ Mev,} \\ R_{p1} &= 3.12 \text{ g/cm}^2, & \text{for } W = 6.96 \text{ Mev.} \end{aligned}$$

The values of the constant  $\alpha$  characterizing the particular values of  $R_{p0}$  chosen are,

$$\alpha = 0.072, \text{ for Al, } \alpha = 0.26, \text{ for Cu.}$$

It should be noted that the large difference between these values stems from the different choices of the standard range  $R_{p0}$  for aluminum and copper. The integral in Eq. (5) is evaluated over a smaller range of energy for copper than for aluminum. The trajectory length,  $x - x_0$ , is consequently smaller which yields a smaller  $\langle \theta^2 \rangle_{\text{Av}}(x-x_0)$  for copper of which  $\theta^2$  is a larger fraction. Introduction of these quantities into Eq. (6) yields  $R_p(E)$  in terms of the standard range  $R_{p0}$ . The solid curves of Fig. 4 were computed in this fashion for aluminum and copper.

The computation described is empirical to the extent that its importance lies only in demonstration that the dependence of scattering probabilities on electron energy is such as to bring the computed range vs. energy curve into agreement with experimental points. The results

reported in Part I are thereby seen to be consistent with the theoretical ionization loss in the region of energy involved. It is possible to find a multiplicative correction term of the form,  $1 - (E - E_0)$ , which yields very nearly as satisfactory agreement with data as does Eq. (6). Such a correction, however, would be purely empirical, whereas that of Eq. (6) was obtained through consideration of the actual reduction in  $R_p$  expected on the basis of elastic scattering theory. The

important point is that the measurement of electron range (and, hence, of energy) by extrapolation of the absorption curve to zero intensity yields approximate values, the error in which increases with electron energy.

The authors are indebted to Dr. W. A. Fowler of the California Institute of Technology for helpful comments regarding possible experimental errors and to Dr. W. F. G. Swann, director of the Bartol Research Foundation, for his interest and frequent advice.

Remarks on the Magnetic Scattering of Neutrons\*

H. EKSTEIN

*Armour Research Foundation of Illinois Institute of Technology, Chicago, Illinois*

(Received January 26, 1950)

The formal calculation of the scattering of neutrons by a magnetized atom leads to a result which is ambiguous in the forward direction. It is shown that, if this singularity is correctly taken into account, apparent discrepancies between macroscopic and atomistic calculations are eliminated.

FOR the calculation of the refractive index of a neutron wave in a ferromagnetic crystal, two different methods have been used with different results.<sup>1-3</sup> The following remarks attempt to explain this discrepancy.

I.

According to Schwinger<sup>4</sup> the amplitude of a neutron beam of spin state  $\chi_0$  scattered elastically by an ion of magnetic moment  $\mathbf{m}$  is

$$\psi_{sc} \sim \frac{m \exp(ik_0R)}{2\pi\hbar^2R} \cdot 4\pi\mu\mathbf{s} \cdot \left( \frac{\mathbf{q}(\mathbf{q} \cdot \mathbf{m})}{q^2} - \mathbf{m} \right) \chi_0, \quad (1)$$

where  $\mathbf{q} = \mathbf{k}_0 - \mathbf{k}$  is the difference between the propagation vectors of the incident and scattered waves, and the other symbols have their usual meanings. This expression has a singularity at the point  $\mathbf{k}_0 - \mathbf{k} = \mathbf{q} = 0$ . Consider the case where  $\mathbf{m} \parallel \mathbf{q}$ . If the point  $\mathbf{q} = 0$  is approached on a sphere  $k^2 = k_0^2$ , the first term in the bracket vanishes. If this point is approached along a line  $\mathbf{k} \parallel \mathbf{k}_0$ ,  $\psi_{sc}$  vanishes, so that the forward scattering is ambiguous in this case.

To find the forward scattering unambiguously, we consider the more general expression for the Born approximation

$$\psi_{sc} = \frac{-\mu m \cdot 4\pi\mathbf{s}}{2\pi\hbar^2} \cdot \int \frac{\exp[ik_0|\mathbf{R} - \mathbf{r}|]}{|\mathbf{R} - \mathbf{r}|} \mathbf{B}(\mathbf{r}) \times \exp[i\mathbf{k}_0 \cdot \mathbf{r}] \chi_0 d\mathbf{r} \quad (2)$$

valid for finite distances  $\mathbf{R}$  from the nucleus.  $\mathbf{B}(\mathbf{r})$  is the magnetic field of the ion. In momentum space, Eq. (2) is

$$\psi_{sc} = \frac{-\mu m \cdot 4\pi\mathbf{s}}{2\pi^2 \cdot 2\pi\hbar^2} \cdot \lim_{\delta \rightarrow 0} \int \frac{\exp(i\mathbf{p} \cdot \mathbf{R})}{p^2 - (k_0 + i\delta)^2} \mathbf{b}(\mathbf{k}_0 - \mathbf{p}) d\mathbf{p} \cdot \chi_0, \quad (3)$$

where

$$\mathbf{b}(\mathbf{q}) = \int \exp(i\mathbf{q} \cdot \mathbf{r}) \mathbf{B}(\mathbf{r}) d\mathbf{r} = 4\pi \left( \frac{-\mathbf{q}(\mathbf{q} \cdot \mathbf{m})}{q^2} + \mathbf{m} \right). \quad (4)$$

Equation (3) can be verified by substituting Eq. (4) and integrating with respect to  $\mathbf{p}$ . In evaluating Eq. (3) for large distances  $|R|$  ( $\mathbf{R} \parallel \mathbf{k}_0$ ) care must be used because of the singularity at  $\mathbf{p} = \mathbf{k}_0$ . The series expansion

$$\begin{aligned} & \int \frac{\exp(i\mathbf{p} \cdot \mathbf{R})}{p^2 - (k_0 + i\delta)^2} \mathbf{b}(\mathbf{k}_0 - \mathbf{p}) d\mathbf{p} \\ &= \int_0^\infty \frac{p^2 dp}{p^2 - (k_0 + i\delta)^2} \int_0^{2\pi} d\phi \int_0^\pi \\ & \quad \times \exp(ipR \cos\theta) \mathbf{b}(\mathbf{k}_0 - \mathbf{p}) \sin\theta d\theta \\ &= 2\pi \int_0^\infty \frac{p^2 dp}{p^2 - (k_0 + i\delta)^2} \left( \frac{\exp(ipR) \mathbf{b}(\mathbf{k}_0 - \mathbf{p})}{ipR} \right) \Big|_{\theta=0}^{\theta=\pi} \\ & \quad + \frac{\exp(ipR) d/d\theta [\mathbf{b}(\mathbf{k}_0 - \mathbf{p})]}{(ipR)^2} \Big|_{\theta=0}^{\theta=\pi} + \dots \end{aligned}$$

is acceptable because  $\mathbf{b}$  is continuous on a sphere

\* This work was supported by ONR.

<sup>1</sup> Halpern, Hamermesh, and Johnson, Phys. Rev. **59**, 98 (1941).

<sup>2</sup> O. Halpern, Phys. Rev. **76**, 1130 (1949).

<sup>3</sup> H. Ekstein, Phys. Rev. **76**, 1328 (1949).

<sup>4</sup> J. S. Schwinger, Phys. Rev. **51**, 544 (1939).